

Article

# Use of Intensity Analysis to Characterize Land Use/Cover Change in the Biggest Island of Persian Gulf, Qeshm Island, Iran

Ali Kourosch Niya <sup>1</sup>, Jinliang Huang <sup>1,\*</sup>, Hazhir Karimi <sup>2</sup>, Hamidreza Keshtkar <sup>3</sup>  and Babak Naimi <sup>4</sup>

<sup>1</sup> Coastal and Ocean Management Institute, College of Environment and Ecology, Xiamen University, Xiamen 361102, China

<sup>2</sup> Department of Environmental Science, Faculty of Science, University of Zakho, Zakho P.O. Box 12, Kurdistan Region, Iraq

<sup>3</sup> Department of Arid and Mountainous Regions Reclamation, Faculty of Natural Resources, University of Tehran, Karaj 31587-77871, Iran

<sup>4</sup> Department of Geosciences and Geography, University of Helsinki, Helsinki 00014, Finland

\* Correspondence: jlhuang@xmu.edu.cn; Tel.: +86-592-2182175

Received: 31 July 2019; Accepted: 12 August 2019; Published: 14 August 2019



**Abstract:** In this study, land use/cover change was systematically investigated in the Qeshm Island to understand how human and nature interact in the largest island of Persian Gulf. Land-use maps were prepared for 1996, 2002, 2008, and 2014 using Landsat satellite imagery in six classes including agriculture, bare-land, built-up, dense-vegetation, mangrove, and water-body, and then dynamic of changes in the classes was evaluated using intensity analysis at three levels: interval, category, and transition. Results illustrated that, while the land changes were fast over the first and third time intervals (1996–2002 and 2008–2014), the trend of changes was slow in the second period (2002–2008). Driven by high demand for construction and population growth, the built-up class was identified as an active gainer in all the three time intervals. The class of bare-land was the main supplier of the land for other classes especially for built-up area, while built-up did not act as the active supplier of the land for other classes. The dense-vegetation class was active in all three time intervals. As for the mangrove class, drought and cutting by residents had negative effects, while setting up protected areas can effectively maintain this valuable ecosystem. High demands were observed for land change in relation to built-up and agriculture classes among other classes. The findings of this study can advance our understanding of the relationship and behavior of land use/cover classes among each other over 18 years in a coastal island with arid climate.

**Keywords:** land use/cover change (LUCC), intensity analysis; Qeshm Island; Persian Gulf

## 1. Introduction

Land use/cover change (LUCC) is regarded as a significant component of global environmental change, and it is mainly linked with regional environmental changes [1]. LUCC results from interaction among various factors such as the economy, housing, employment, environment, etc. Population growth and its distribution has played a key role in acceleration of land-use change in recent centuries [2]. Urban development and land-use pattern change have considerable social and environmental effects including destruction of natural habitats, increased natural hazards, severe watershed erosions, sedimentation in seas (especially in coastal zones), biodiversity loss, water quality reduction, and loss of areas related to suburban farmlands and green spaces. Generally, it can be claimed that, LUCC in coastal zones leads to an increase in the vulnerability over these areas [3,4]. The aforementioned

problems and the consequent hazards are somewhat related to land-use changes caused by human activities, and thus, it is crucial to understand the magnitude and trend of LUCC and its spatial patterns.

Problems resulting from land-use changes are more important and intense in the coastal areas [5], which can be regarded as an intersection between three different environments; atmosphere, hydrosphere, and lithosphere [6]. This issue calls for more attention and supervision on coastal zones given their limitations and special conditions. Despite the attempts made to protect the coastal regions, the uncontrolled exploiting of coastal resources has resulted in destruction of the resources, emergence of serious threats, and challenges to these valuable ecosystems [7]. These consequences have sometimes been irreversible, especially in the case of biosphere reserves [8].

Undoubtedly, the first step towards sustainable usage and protection of these areas is a precise understanding and monitoring of land-use changes. However, monitoring and analyzing of land-use changes using in-situ and field methods is time consuming and costly. Therefore, to analyze and understand LUCC, it is necessary to use proper technologies and innovative measurement methods [9,10] such as remote sensing (RS) and geographical information systems (GIS). Utilization of these powerful technologies not only accelerates the process, but also provides a thorough understanding of status and trend of each land-use class over time and reveals the relationships between different classes [11]. It is expected that, the use of these techniques for analysis of the existing regional land-use changes would help specialists to prepare and implement management plans regarding sustainable developments [12].

A traditional land-use changes matrix is not adequate for achieving quantitative and systematic LUCC feedbacks, and there have been attempts to further clarify substantial causes and processes of land-use change using the transition matrix analysis method [8]. Intensity analysis is one of these methods, which in fact, provides a quantitative framework for calculation of similar class changes during different periods constituting the rows and columns of a square transition matrix [13–15]. As a quantitative approach, this method was developed by Clark University to assess land-use changes based on land-use classes in the following three levels: time interval, category, and transition. Land-use change analysis during specific periods is the most common application of this method [16]. This approach can identify the deviation in all of the mentioned areas in range of the observed changes and hypothesized uniform changes [13,17]. By applying the intensity analysis, the observed intensities of LUCC can be calculated and compared with a uniform intensity among different land use/land cover (LULC) classes [14].

Intensity analysis is very effective in determining the size and strength of changes in various land categories over time intervals between the observed changes and supposed uniform changes. Intensity analysis can detect pattern of changes in which changes are constant or variable during different time intervals to make a better understanding of the process of land-use changes [17,18]. Due to these abilities, numerous studies have investigated the temporal and spatial process of LULC using intensity analysis. For example, Zhou et al. (2014) analyzed land-use changes at three levels: time interval, category, and transition in Jiulong River watershed in China using intensity analysis method [17]. Akinyemi et al. (2016) investigated the land-use changes using intensity analysis in Kigali, Rwanda in a 25-year period [18]. Shoyama et al. (2018) analyzed the effects of crop expansion on natural vegetation distribution using intensity analysis in northern Ghana in three time intervals (from 1984 to 2015) [19]. Da et al. (2019) characterized the spatiotemporal changes of land use/land cover in the Shule river basin using the intensity analysis [20]. Huang et al. (2018) compared intensity analysis and the land-use dynamic degrees' methods, and analyzed the land-use changes in the coastal zone of Longhai in Southeast China [21].

Qeshm Island suited in south of Iran at the intersection of the Persian Gulf and the Oman Sea, plays an important role as a free trade zone in the economy of Iran [22]. Besides its strategic position, this island is also one of the unique tourist attractions of Iran and has a unique marine and terrestrial environment. However, recent decades, the ecological environment and ecosystem of the coastal area have been deteriorated due to urbanization and significant economic developments. In order to

understand the extent and distribution of changes, it is necessary to investigate and assess the trend of LUCC in space and time in this island. Thus, the intensity analysis was used in this study to measure the spatiotemporal changes of LULC in Qeshm Island. To our knowledge, our study is the first that applied this method at a local scale in the south of Iran. This study would be an example that links the patterns of land-use changes to the processes, thus providing a spatial basis for land-use policy and decision-making based on sustainable development to protect the island environment.

## 2. Materials and Methods

### 2.1. Study Area

Case under study is the Qeshm Island situated in the south of Iran close to the Strait of Hormuz in the Persian Gulf (Figure 1) from  $55^{\circ}14'58''$  E to  $56^{\circ}17'27''$  E and from  $27^{\circ}00'00''$  N to  $26^{\circ}32'04''$  N. As the country's biggest free trade zone with respect to the landmass [23], Qeshm is one of the most densely populated islands in Iran, with an area of 1491 square kilometers, approximately two times bigger than Bahrain as the second largest island in the Persian Gulf [24].

Qeshm Island has great landscape diversity representing great ecological richness due to its unique environment in the Persian Gulf [25]. Due to particular environment of the Qeshm, in 2006, UNESCO introduced this island as the first geo-park in the Middle East [26]. Beautiful coral reef colonies, the largest Mangrove community in Iran, and its integration with historical places has created tourism attractions in the island. In addition, active ports, fisheries, and different commercial activities have been shown to highly influence economic performance of this area.

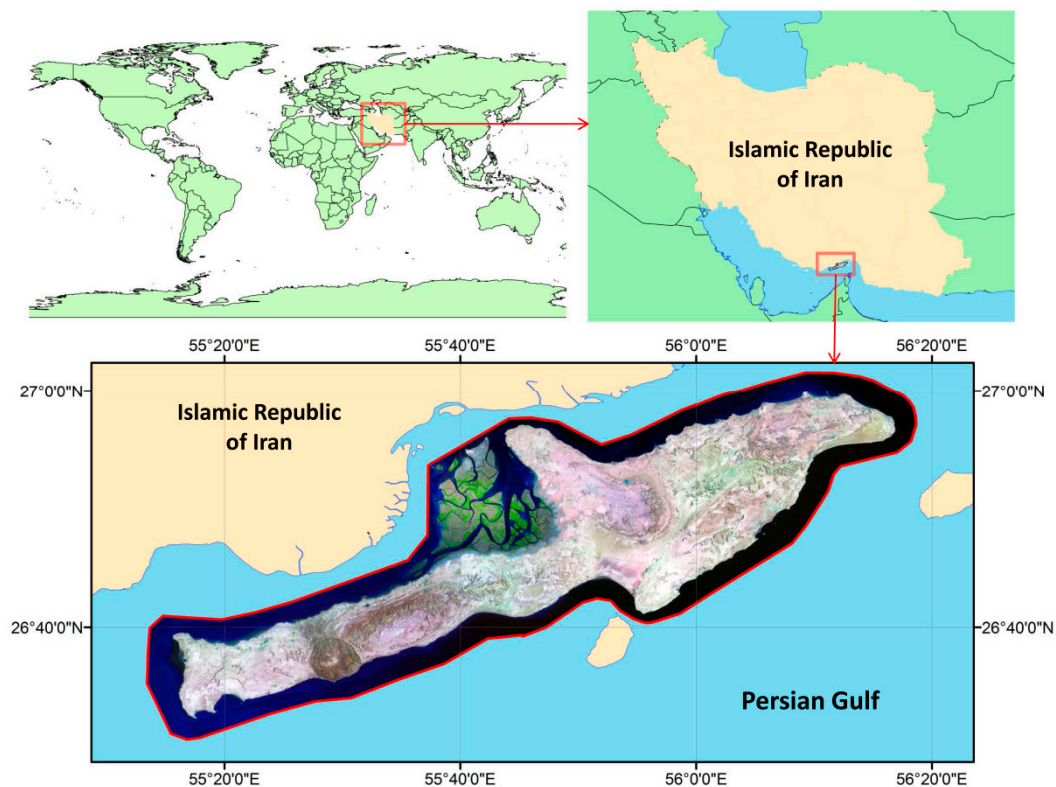


Figure 1. Location of the study area located in south of Iran.

### 2.2. Data

Landsat series of images including Landsat 5, 7, and 8 have been used in this research. All satellite images (a total of eight scenes) have downloaded from USGS archive (<http://earthexplorer.usgs.gov>) [27]. Table 1 shows specifications of images including the satellite, sensors, path, row, and acquired date.

Lack of cloud cover, time synchronization, and being near to the season of precipitation were considered in selection of these images. Also, a topographic map of Qeshm Island generated by Iran's National Cartographic Center at the scale of 1:25,000 and the Google Earth images were used to extract training data.

**Table 1.** List of Landsat satellite images used in the research.

No.	Satellite	Sensors	Path	Row	Date
1	Landsat5	Thematic Mapper (TM)		041	16 May 1996
2	Landsat5	Thematic Mapper (TM)		042	16 May 1996
3	Landsat7	Enhanced Thematic Mapper Plus (ETM+)		041	25 May 2002
4	Landsat7	Enhanced Thematic Mapper Plus (ETM+)	172	042	9 May 2002
5	Landsat5	Thematic Mapper (TM)		041	17 May 2008
6	Landsat5	Thematic Mapper (TM)		042	17 May 2008
7	Landsat8	Operational Land Imager (OLI)		041	18 May 2014
8	Landsat8	Operational Land Imager (OLI)		042	18 May 2014

### 2.3. Preparing LULC Maps

In this study, a combination of on-screen digitizing and supervised classification was used to prepare LULC maps during the years of 1996, 2002, 2008, and 2014. So that, in data collection phase, Landsat images were selected (level 1 products) and downloaded from the USGS archive knowing that the images lacked cloudiness, dates of the images were close to plant growing season, and there were no or slight intervals between the dates.

In the preprocessing phase, the study area was identified on the images, and it was masked based on different image layers. Afterward, to use all the image bands in the classification process, different bands of each image were combined using the 'layer-stacking' command and the mosaic of images was created for further processing. In the processing stage, initially 6 LULC classes were described as presented in Table 2, and then to increase accuracy of the output maps, built-up and agriculture classes were extracted using Google Earth, topographic maps, aerial imagery, and the pan-sharped Landsat images.

**Table 2.** List of LULC classes and description for each class.

No.	Class Name	Description
1	Agriculture	Land used for cultivation including orchards, cultivated land of all kinds of agricultural products.
2	Bare-land	Unused land, including barren land, wild grass ground, alkaline land, wetland, sand, waste land.
3	Built-up	Residential area, including urban, rural, industrial, all kinds of road, airport, surrounded enterprise area and generally human-made area.
4	Dense-vegetation	Densely covered vegetation range is recognizable on Landsat which are outside the range of the built-up and agriculture classes.
5	Mangrove	The range of mangroves, both natural and artificial.
6	Water-body	Includes sea area and water bodies inside the island.

Then, masks were prepared for the two extracted classes, and supervised classification was used to automatically extract four other classes including dense-vegetation, mangrove, water body, and bare-land from the images. Maximum likelihood classification method, which is still one of the most common supervised classification algorithms [28] was used at this stage. To conduct a supervised classification of satellite images, the training data must be determined precisely. Selection of the training data is the most challenging and critical part of the supervised classification method [29–31]. The training points were obtained using Google Earth images, topographic maps (including maps of constructed lands, roads, and airports), and Landsat pan-sharped images. Then, six extracted classes

were combined to prepare four time intervals in the GIS environment, and final maps were provided for change detection step. Finally, to verify results of this step, error matrix as the most common method of evaluating accuracy regarding using remote sensing data [32] was formed to measure accuracy of the maps. This matrix is the result of a comparison between the pixels including known pixels or ground control pixels with the corresponding pixels in the classification results. Figure 2 illustrates the overall framework of this study.

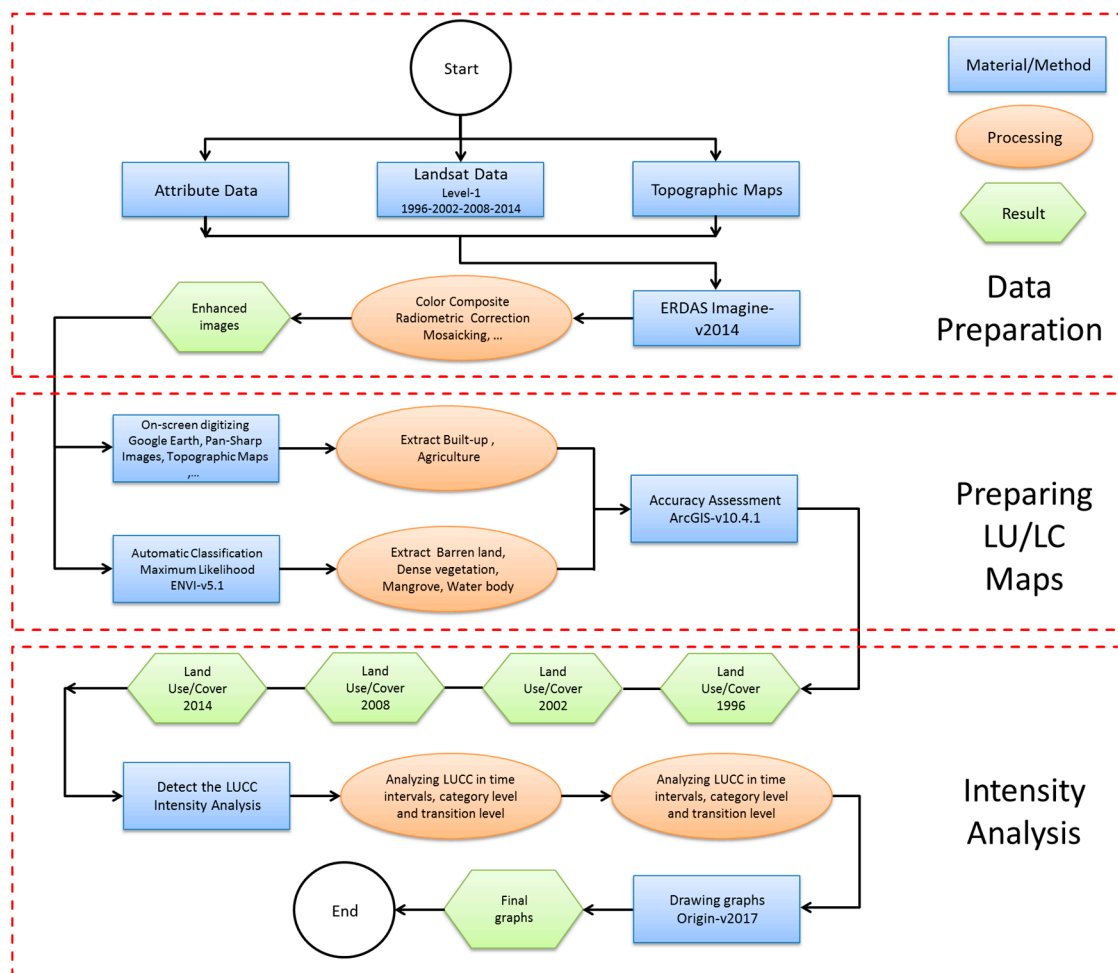


Figure 2. Flowchart of the study.

#### 2.4. Intensity Analysis

Amounts of land-use changes are visible in the framework of traditional changes; but, a more profound investigation is necessary in order to describe the linkage between patterns in different classes with the corresponding processes [33]. Intensity analysis is a complex method, providing the possibility of doing more detailed investigation for the researchers. This approach is a computational framework to demonstrate interactions between categorical factors during the time intervals as well as quantifying the grade and intensity where changes are non-uniform in different levels of details [13,34,35]. According to advantages of the intensity analysis and regarding the fact that, whether an occurred transition from one class of land-use to another class deviates from a uniform operation, it can be acknowledged that this method is important for analyzing land-use changes. Intensity analysis takes place at three levels including time intervals, category, and transition.

The time interval corresponds to overall changes within one specific interval compared to the overall changes within other interval(s). Then, any changes in gross loss/gain intensity among different categories are separately described by the category level during time intervals, the extent to which

the level of changes is an indicator of how the intensity would change. Such change results from a specific category of changes among other categories during each time interval [13–18]. With regard to the study by Aldwaik and Pontius, our analysis is based on five equations as notated in Table 3.

Pace of transitions in an interval is calculated based on Equation (1), by dividing size of the transition by length of the time interval resulting in a percentage of spatial extent. A category's yearly gross loss intensity in an interval is obtained by Equation (2), by dividing the size of the category's yearly gross loss by the size of the category at the starting point of each interval. Using Equation (3), a category's yearly gross gain intensity in an interval is determined; to this end, the size of the category's yearly gross gain is divided by the size of the category at the final stage of each time interval. Common hypothesis regarding the category level for each interval suggests that, all categories undergo gross loss and gross gain with the same yearly intensity. This amount is equal to pace of transition in the interval, in other words,  $S_t$ . In case  $L_{ti} < S_t$ , the loss of  $i$ , is stopped all along the interval  $t$ ; quite similarly, if  $G_{tj} < S_t$ , it means that gain of  $j$  is withheld within the interval  $t$ . In the case  $L_{ti} > S_t$ , loss of  $i$  is considered active along the interval  $t$ ; consequently, if  $G_{tj} > S_t$ , gain of  $j$  is called active within that time interval.

**Table 3.** Mathematical notation following Aldwaik and Pontius (2012).

Symbol	Description
$T$	number of time points
$Y_t$	year at time point $t$
$t$	index for the initial time point of an interval $[Y_t - Y_{t+1}]$ , where $t$ ranges from 1 to $T - 1$
$J$	number of categories
$i$	index for a category at the initial time point of an interval
$j$	index for a category at the latter time point of an interval
$n$	index of the gaining category for the selected transition
$C_{tij}$	size of transition from category $i$ to category $j$ during interval $[Y_t - Y_{t+1}]$
$S_t$	annual change during interval $[Y_t - Y_{t+1}]$
$G_{tj}$	intensity of annual gain of category $j$ during interval $[Y_t - Y_{t+1}]$ relative to size of category $j$ at time $t + 1$
$L_{ti}$	intensity of annual loss of category $i$ during interval $[Y_t - Y_{t+1}]$ relative to size of category $i$ at time $t$
$R_{tin}$	intensity of annual transition from category $i$ to category $n$ during interval $[Y_t - Y_{t+1}]$ relative to size of category $i$ at time $t$
$W_{tn}$	uniform intensity of annual transition from all non- $n$ categories to category $n$ during interval $[Y_t - Y_{t+1}]$ relative to size of all non- $n$ categories at time $t$

$$S_t = \frac{\text{Change during } [Y_t, Y_{t+1}]}{(\text{Duration of } [Y_t, Y_{t+1}])(\text{Extent Size})} 100\% = \frac{\sum_{j=1}^J [(\sum_{i=1}^J C_{tij}) - C_{tij}]}{(Y_{t+1}, Y_t) \left( \sum_{j=1}^J \sum_{i=1}^J C_{tij} \right)} 100\% \quad (1)$$

$$L_{ti} = \frac{\text{Annual loss of } i \text{ during } [Y_t, Y_{t+1}]}{\text{Size of } i \text{ at } Y_t} 100\% = \frac{[(\sum_{i=1}^J C_{tij}) - C_{tij}] / (Y_{t+1} - Y_t)}{\sum_{j=1}^J C_{tij}} 100\% \quad (2)$$

$$G_{tj} = \frac{\text{Annual gain of } j \text{ during } [Y_t, Y_{t+1}]}{\text{Size of } j \text{ at } Y_{t+1}} 100\% = \frac{[(\sum_{i=1}^J C_{tij}) - C_{tij}] / (Y_{t+1} - Y_t)}{\sum_{i=1}^J C_{tij}} 100\% \quad (3)$$

$$R_{tin} = \frac{\text{Annual transition from } i \text{ to } n \text{ during } [Y_t, Y_{t+1}]}{\text{Size of } i \text{ at } Y_t} 100\% = \frac{C_{tin} / (Y_{t+1} - Y_t)}{\sum_{i=1}^J C_{tij}} 100\% \quad (4)$$

$$W_{tn} = \frac{\text{Annual gain of } n \text{ during } [Y_t, Y_{t+1}]}{\text{Size of non-} n \text{ at } Y_t} 100\% = \frac{[(\sum_{i=1}^J C_{tin}) - C_{tnn}] / (Y_{t+1} - Y_t)}{\sum_{j=1}^J [(\sum_{i=1}^J C_{tij}) - C_{tnj}]} 100\% \quad (5)$$

Equation (4) determines the intensity of annual transition of the gain of a specific category  $n$  from other categories  $i$ , that is the quantity of the yearly transition to the specific category  $n$  from the other category divided by quantity of another category at starting point of each interval. The predominant hypothesis at the level of transition for intervals suggests that specific category  $n$  transitions to all other categories with a similar yearly intensity [18]. This amount is calculated by Equation (5), by dividing the size of the yearly gain of category  $n$  by the total amount of sizes of all other categories at the starting point of time intervals. Therefore, if  $R_{tin} < W_{tn}$ , hence gain of  $n$  stops  $i$  all along interval  $t$ . In case  $R_{tin} > W_{tn}$ , then, gain of  $n$  targets  $i$  within interval  $t$ . A comprehensive description of intensity analysis was given by Aldwaik and Pontius [18,34]. There are also case studies in which intensity analysis has been applied including Southeast China [4,8,17], Rwanda [18], Indonesia [16], and Southern Nigeria [35].

### 3. Results

#### 3.1. Land Use/Cover Maps

The land-use maps of Qeshm Island (Figure 3), prepared using the integration of on-screen digitizing and the supervised classification (maximum likelihood), were classified in six classes and as it is visible on the map, the most area of Qeshm Island belongs to the bare-land class. In addition, the maps show that the built-up areas are mostly located around the coastline. Furthermore, the mangrove forest is visible in central north part of the island.

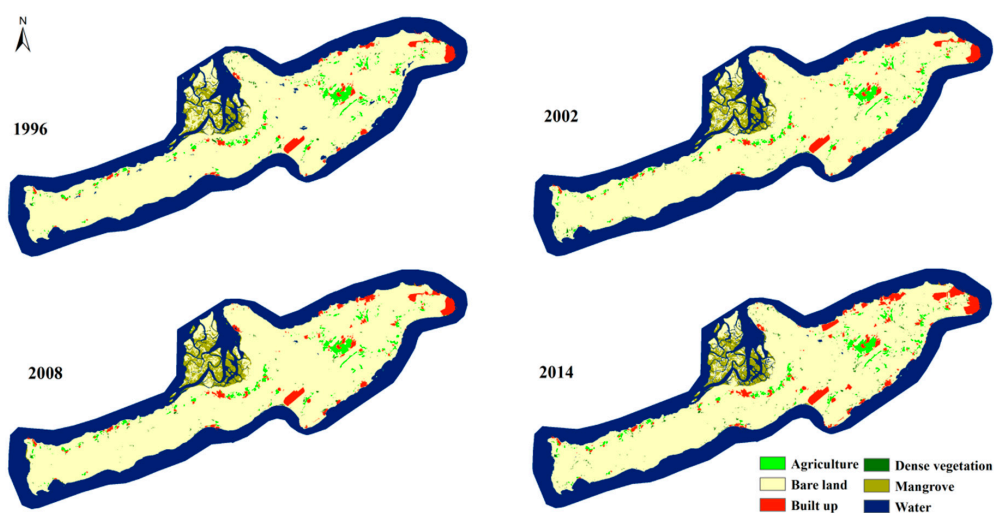


Figure 3. Land-use maps for study time interval in six classes.

The matrix of variations in land-use classes (Table 4) that was prepared based on the number of pixels belong to each class illustrates that the built-up is the only class upgraded in each period, so that, 6954 and 24,326 pixels were changed in the first and second periods, respectively in this class among other classes. In fact, this class showed an increase by more than 34% in the final year compared to the initial one, as a result of the development plans in the Qeshm Free Trade Zone. On the other hand, during the time of the study, only 24 pixels of this class have been changed to agriculture and bare-land classes. At the same time, the bare-land class is the only class experienced a decrease in each time interval, due to vast expanse of this class in Qeshm Island and lower legal limits for changing this class of land-use to other classes. The reduction of the agriculture class in the first period is another remarkable point in the table, which by the way has happened in a small amount (250 pixels in total). Also, the increment in the mangroves level due to protective actions and artificial implantation of mangroves in the first period and also its reduction in the second period, probably due to periods of drought in this region during this period [36] is another important point in the table.

**Table 4.** Variation matrix for each land-use class based on the number of pixels.

		2014						
	Categories	Agriculture	Bare-land	Built-up	Dense-vegetation	Mangrove	Water-body	Total
2008	Agriculture	46,966	1266	415	686	0	0	49,333
	Bare-land	4122	1,502,515	22,951	11,247	2594	7565	1,550,994
	Built-up	0	0	66,958	0	0	0	66,958
	Dense-vegetation	864	1144	30	3890	443	70	6441
	Mangrove	0	3104	0	13	69,600	10,942	83,659
	Water-body	1	6376	930	0	915	1,002,535	1,010,757
	Total	51,953	1,514,405	91,284	15,836	73,552	1,021,114	2,768,142
		2008						
	Categories	Agriculture	Bare-land	Built-up	Dense-vegetation	Mangrove	Water-body	Total
2002	Agriculture	47,252	1450	510	370	0	1	49,583
	Bare-land	1958	1,536,543	5978	3355	3672	1483	1,552,989
	Built-up	2	22	59,980	0	0	0	60,004
	Dense-vegetation	121	6629	90	2381	130	5	9356
	Mangrove	0	1565	0	328	73,535	383	75,811
	Water-body	0	4785	400	7	6322	1,008,885	1,020,399
	Total	49,333	1,550,994	66,958	6441	83,659	1,010,757	2,768,142
		2002						
	Categories	Agriculture	Bare-land	Built-up	Dense-vegetation	Mangrove	Water-body	Total
1996	Agriculture	45,660	5643	19	293	0	0	51,615
	Bare-land	3043	1,531,873	3927	6821	8823	17,278	1,571,765
	Built-up	0	0	55,525	0	0	0	55,525
	Dense-vegetation	813	7049	34	1839	52	0	9787
	Mangrove	41	970	0	21	64,992	648	66,672
	Water-body	26	7454	499	382	1944	1,002,473	1,012,778
	Total	49,583	1,552,989	60,004	9356	75,811	1,020,399	2,768,142

In this research, the total accuracy and also the standard Kappa were used to verify the accuracy of classifications. Accuracy of the maps was evaluated based on 300 control points for each year from the study area using topographic maps, Google Earth, and Landsat pan-sharped images. Then, these points were compared with produced maps, and ultimately, total accuracy and the Kappa coefficient were calculated for the result maps. Accuracy assessment of the maps extracted from the method used in this study showed that, overall accuracy is at least 88% and at most 91%. Also, the Kappa coefficient in the final maps is equal to 0.85, 0.87, 0.86, and 0.89, respectively, for the years 1996, 2002, 2008, and 2014 (Table 5).

**Table 5.** Overall accuracy for the land-use maps.

Year	Error Count	Samples Count	Overall Accuracy	User's Accuracy	Producer's Accuracy	K-Standard
1996	36	300	88.00	89.81	88.00	0.85
2002	32	300	89.33	90.35	89.33	0.87
2008	33	300	89.00	89.72	89.00	0.86
2014	27	300	91.00	90.18	91.33	0.89

### 3.2. Intensity Analysis

According to the transfer matrix of land-use change in three time intervals, total amount of land-use change in each period, annual change intensity, and change intensity in all periods are presented in Figure 4. Each of the bars extending from the center axis to the left shows percentage of change level in time intervals of the study. Also, the bars developed from the center axis to the right express the intensity of the changes in the study periods. As can be seen, total land-use changes were fast during two periods: from 1996 to 2002, and from 2008 to 2014, while changes were slow in the time interval from 2002 to 2008. Accordingly, annual intensity of the changes was evaluated as slow in the period of 2002–2008, and intensity of the changes was evaluated as rapid in the period of 2008–2014. These changes are certainly associated with the policies adapted for development of free trade zones and increasing activities of this region in order to sustain country's economy.



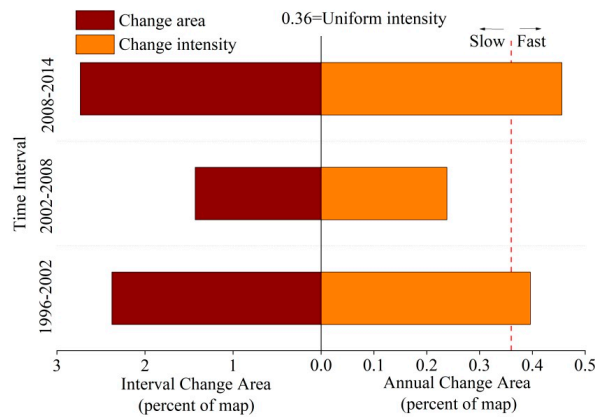


Figure 4. Rate of change in level and intensity of changes in the study area.

Figure 5 shows intensity of the changes in study periods with respect to the land-use classes. As shown in Figure 5, in all three time intervals of the study, intensity of changes in gain and loss was evaluated to be more in the dense-vegetation class than other classes, indicating instability of this class of land-use in the region because of the severe effect of amount and distribution of precipitation on this class. The built-up class is the next class experiencing major changes, due to the high interest of the stakeholders for construction in the study region and development plans in the free economic zone of Qeshm Island. Of course, as noted above, changes in this class of land-use were merely incremental. On the other hand, although bare-land-use changes declined in all periods, and the highest numbers of pixels changed in this class compared to others, but, due to its large area, overall change in this class is not intense.

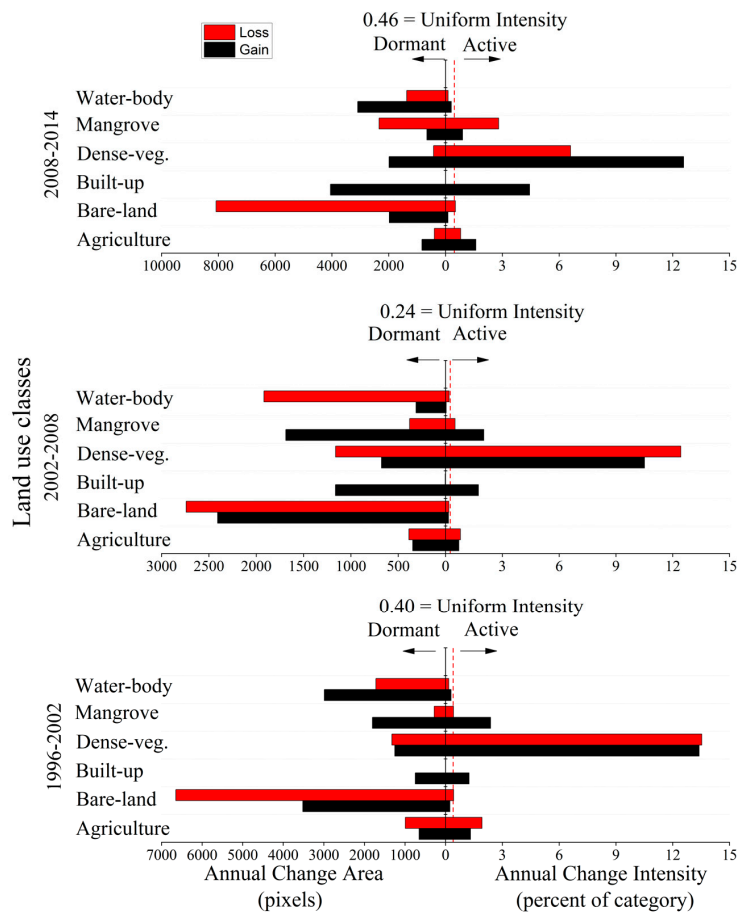


Figure 5. Rate of change in category level and intensity of changes according to land-use classes.

Figure 6 illustrates the intensity of the observed transitions for agriculture, dense-vegetation, and mangrove classes according to the amount of gained pixels for all the three-time intervals. If a bar passes the uniform line in the graph, it indicates that the category’s gain targets the losing category, while stopping a bar before the uniform line indicates that the category’s gain avoids the losing category. As it appears in graphs, valuable classes (built-up and agriculture) have no active role as a supplier of land for other classes while the bare-land has been main supplier for built-up land in all the three-time intervals. As shown in Figure 6, bare-land and dense-vegetation tend to be main targets of mangrove loss in the first and second periods; however, in the third period, water-body gained more intensively than bare-land and dense-vegetation classes. Bare-land tends to be targeted more intensively by the built-up than other classes in all the three periods.

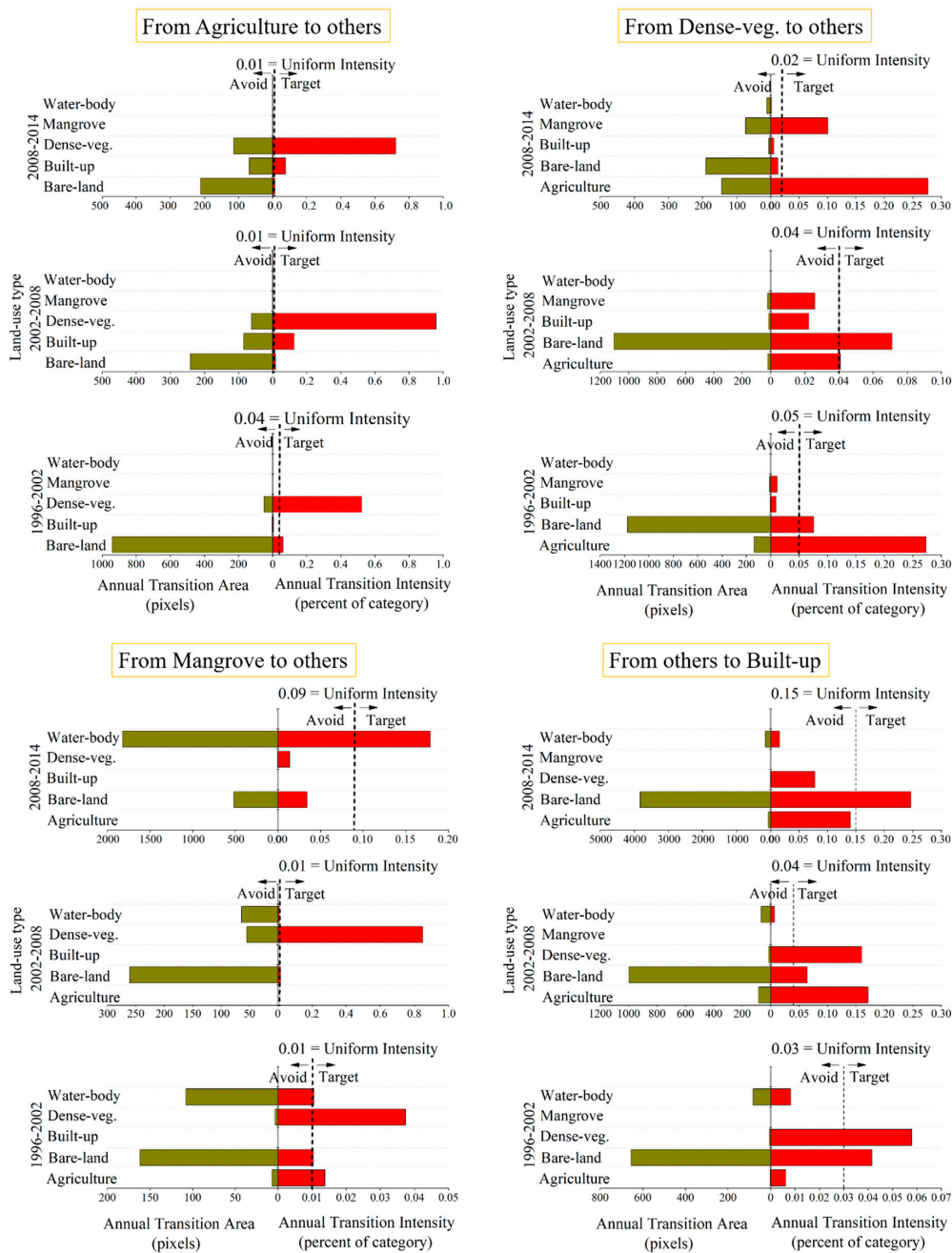


Figure 6. Transition intensity given category gains during three-time intervals.

## 4. Discussion

### 4.1. Patterns to Processes in LUCC

Qeshm Island with its unique environment plays an important role in country's economy, but it has faced severe land-use changes during recent years. Intensity analysis method was used in this study to analyze transition of changes among land categories during three time intervals in this island. Previous studies conducted in Iran have not yet used the intensity analysis method for LULC studies; however, some studies in other countries have applied this method and analyzed LULC patterns in three levels: interval, category, and transition, especially in the coastal areas. These studies have found that process of land-use change has happened quickly in the coastal areas, and proposed insights into patterns and the underlying processes of LUCC similar to our research.

Time intervals analysis indicated that, overall land-use change was faster in the first (1996–2002) and third time intervals (2008–2014) than the second time interval (2002–2008). Recent significant development, and economic growth of the Qeshm Island have accelerated these changes. Overall policy of the country has made this island an economic and strategic pole in the region. Several studies concluded findings similar to our study in terms of time interval analysis. For instance, Zuo et al. (2011) analyzed the land-use changes of several coastal cities in China and found that, the first interval has experienced smaller land-use change rate compared to other intervals [37]. Huang et al. (2012) quantified intensity of land-use changes during three time points (1986–1996, 1996–2002, and 2002–2007) in the coastal watershed of southeast China [8]. They concluded that, intensity of land-use change is associated with intensity of development in the study area.

Intensity analysis at the category level showed that, the built-up class has been an active gainer during each of the three time intervals and has separated sections of other land-use classes. This can be justified by rising demand for construction and converting the lands to built-up areas. The agriculture class is important from two perspectives. On the one hand, agriculture is classified as a built-up margin that has been on the verge of becoming a built-up class, and on the other hand, it is of high value as supplier of required food supplies (especially given the limited area for preparing agricultural land), that is protected by local government. However, high demand for construction and high value of the land on the island has led to the largest change of agriculture class to the built-up class. Previous studies conducted on land-use changes in coastal areas are in good agreement with our findings. For instance, Yang et al. (2017) characterized the land-use changes in Zhenlai County in the northeast of China. They concluded that, the most prevalent changes happened in built-up lands mainly influenced by economic and political reasons, while arable lands experienced less intensively gains and losses [38]. Huang et al. (2018) measured the land use changes in coastal zones around urban areas that have experienced rapid growth in China. They reported similar results, so that they found that the urbanization, built-up gains, and cropland losses were active for all time intervals [4].

Analysis of intensity of changes in the three periods indicated high level of change in dense-vegetation class, attributing to high dependence and direct relation of this class to extent of precipitation and rainfall instability in the arid and ultra-arid climates. This has been especially evident from several droughts in the region as shown in the study by Mafi-Gholami (2017), who showed that the SPI index has been significantly less compared to previous years [36]. Also, the mangrove class showed significant changes compared to other classes. On the one hand, being recognized as the protected area may protect this ecosystem and, on the other hand, natural factors and direct (cutting the trees by local people) and indirect (marine transportation and pollution into the sea) human uses cause damages to mangrove trees. Results of the present study revealed that the above-mentioned resultant factors increased area of the mangrove class in the first and second time intervals and decreased area of this class in the third period, as confirmed in the study conducted by Khoorani et al. (2015), who indicated an average increasing rate (18.28 hectares per year) for the mean change in the breadth of mangroves in the Khamir and Qeshm habitat zones between 1984 and 2009 [39].

In terms of transition intensity, analysis showed some differences in the transitioned class and the year. The transition from bare-land to built-up, bare-land to agriculture, bare-land and agriculture to dense-vegetation, and dense-vegetation to mangrove has been the target for all three time intervals. However, transition rate from water-body and mangrove to agriculture and built-up classes were zero in all three periods. The mangrove forest is protected by both local and international conservation efforts, and protection alarms of the mangrove ecosystem have been increased in recent years. Also, due to high value of land and construction costs, transition from built-up and agriculture classes to other classes has been zero in three periods. However, lands surrounding the urban areas are used for agriculture, which resulted in transition from agriculture to built-up in Qeshm Island. Therefore, urban expansion occurs mostly adjacent to the cultivated lands. Some studies conducted in the coastal regions showed a similar pattern so that, spatial increase in the residential regions has been found to be usually accompanied by loss of agriculture lands [2,8,37,40].

Intensity analysis technique was applied in this study to characterize LULC changes in the study area. Intensity analysis is a powerful method used to characterize LULC changes among categories over time [41]. Various studies have used methods such as Markov transition matrix-based and the land-use dynamic degree to characterize land-use changes among categories over the time. However, these methods are neither particularly helpful to understand patterns of land-use changes nor show size of category loss and gain. Some researchers have compared intensity analysis with other methods. Aldwaik and Pontius (2012) compared the intensity analysis and Markov-based transition matrix [13]. They reported that intensity analysis is much more effective in additional analysis and explain matrices in more details in consecutive time intervals than Markov matrices. Also, Huang et al. (2018) compared intensity analysis and land-use dynamic degrees to quantify temporal change among categories in China's southeast coastal region [4]. They found that, comprehensive land-use dynamic degree (CLUDD) cannot show size and intensity of changes at consecutive levels, while intensity analysis spatially characterizes changes in three levels of time, category, and transition.

#### 4.2. Driving Forces of LUCC

Since 1996, intensive changes in land use/land cover change have been undoubtedly influenced by formation of the Qeshm Free Zone Organization in the early 1990s. The government approved establishment of Qeshm Free Trade Zone to utilize economic potential of Qeshm Island and create economic mobility. As a result of this decision and increasing amount of investment and carrying out industrial activities, and ultimately due to rapid development in this area, man-made land-use changes have also increased because of economic activities, rapid developments, and domestic and international investments over the recent years, as supported in the study by Hakimian (2009) [42]. Findings of our research showed patterns and processes of LUCC associated with economic growth and human activities similar to other studies conducted in many other coastal areas [8,17].

Recent economic developments followed by the increase in the population are among crucial driving forces of the LUCC in Qeshm Island. Pressure of population increase in Qeshm Island, beyond the indigenous population living in the region is due to high level of positive net migration to the island as a result of the economic activities. According to the National Census, the population in the study area has increased from 73,000 in 1996 to 149,000 in 2016, meaning that the Qeshm population has been more than doubled over 20 years ago [43]. Moreover, a large number of visitors travel to Qeshm Island daily due to tourism and economic attractions [44]. Significant population growth led to major land conversion to built-up and agriculture areas in order to provide food needs of local inhabitants.

Also, natural factors have adverse effects on LUCC in the study area. Climate situation is a primary influential factor in relation to LUCC in Qeshm Island. Increasing annual average temperature and decreasing annual precipitation have directly influenced the mangrove ecosystems in the study area. In the last century, the SPI value and annual rainfall have decreased and led to frequent droughts in Qeshm Island as reported in the study by Mafi-Gholami et al. (2017) [36]. They investigated the

relationship between drought events and mangrove in the study area and found that mangrove areas are significantly related to the reduction in the annual rainfall and occurrence of more drought events. Khorani et al. (2015) confirmed that the areas of mangrove forests experienced fluctuations in a 25-year period from 1985 to 2009. They found that meteorological parameters have a significant relationship with changes in the areas. Other causes such as changes of seawater salinity, sea levels, and human activities incorporated with climate change may have intensified climatic effects [39].

It is essential to preserve and manage the sustainable plans of coastal zones in order to decrease destruction of mangrove habitats and create a balance between environmental conservation (mangrove) and economic development (urbanization) in Qeshm Island. Environmental management plans should create a good balance between conservation plans and land utilization and be achievable in both short- and long-term programs. Achievable and useful programs may be realized through assessment of environmental effects related to implementation of the projects, participation of local inhabitants in protection projects, estimation of country and region necessities, and consideration of land-use related planning in development plans. In addition, it is possible to present approaches for planning and ecological design of mangrove habitats in Qeshm Island based on the human awareness. Maintaining moisture balance in warm and humid areas is an essential principle regarding specific climate protection in deserts [45,46]. Mangrove forests are of aesthetic value for the region and country. Therefore, it is necessary to consider sustainable tourism principles compatible with ecosystem sensitivity in developing tourism plans in this island based on the principles of sustainable development of tourism.

## 5. Conclusions

In this study, remote sensing, GIS, and intensity analysis were used together within an integrated framework to analyze the changes and dynamics of LUCC in Qeshm Island as the largest island in the Persian Gulf. The intensity analysis and changes were evaluated for six classes of land-use and at three levels: time, category, and transition. This study showed that the intensity analysis method can facilitate and provide informative signals of land changes as were practiced in the biggest island in the Persian Gulf.

Three time intervals in this study showed significant differences. Total land-use changes were found to be accelerated in the first and third periods (1996–2002 and 2008–2014), while there was a slowdown in the interim period, from 2008 to 2014. Economic and investment factors in the region were the most important human factors, and drought was as the most important natural factor with a decisive role in the LUCC changes. Generally, changes in the studied periods were due to demand for built-up and agriculture classes in order to take the advantage of the local opportunities, and most of the land areas have been separated from the bare-land class, given the legal ease, and converted into two mentioned classes and other classes. Also, the dense-vegetation class has been mostly changed among all classes due to high effect of rainfall instability on this class. Transition level that measures intensity variation showed that the bare-land class was intensively losing more space to built-up than other classes, while dense-vegetation tends to be main target of mangrove loss. Transition from agriculture and built-up to other classes were zero or near the zero due to their high economic value over three periods. Also, the mangrove class did not have any role in provision of land for the built-up class because of being in the protected area.

Land use/cover patterns in the study area can be considered as the outcomes of human and nature interactions, that can reflect the underlying human activities (e.g., urbanization and environmental conservation) on local natural conditions (e.g., climate and topography). In this case, the arid climate in Qeshm Island determines the unique characteristics of vegetation dynamics; the coastal location and local policy has driven land change over 18 years. It will be interesting to perform comparative studies with other areas with different climatic zones and in different regions.

**Author Contributions:** A.K.N. and J.H. conceived and designed the project; A.K.N. and J.H. executed analyses; A.K.N., J.H., H.K. (Hazineh Karimi), H.K. (Hamidreza Keshtkar), and B.N. wrote the paper.

**Funding:** This research was supported by Chinese Government Marine Scholarship (Grant No. 2016SOA016).

**Acknowledgments:** Anonymous reviewers supplied constructive feedback that helped to improve this manuscript.

**Conflicts of Interest:** The authors declare no conflict of interest. The funding sponsors had no role in the design of the study; in the collection, analyses, or interpretation of data; in the writing of the manuscript, or in the decision to publish the results.

## References

- Mendoza-Poncea, A.; Corona-Núñez, R.; Kraxner, F.; Leduca, S.; Patrizio, P. Identifying effects of land-use cover changes and climate change on terrestrial ecosystems and carbon stocks in Mexico. *Glob. Environ. Chang.* **2018**, *53*, 12–23. [[CrossRef](#)]
- Lambina, E.F.; Meyfroidt, P. Global land-use change, economic globalization, and the looming land scarcity. *Proc. Natl. Acad. Sci. USA* **2011**, *108*, 3465–3472. [[CrossRef](#)] [[PubMed](#)]
- Li, Y.; Zhang, X.; Zhao, X.; Ma, S.; Cao, H.; Cao, J. Assessing spatial vulnerability from rapid urbanization to inform coastal urban regional planning. *Ocean Coast Manag.* **2016**, *123*, 53–65. [[CrossRef](#)]
- Huang, F.; Huang, B.; Huang, J.; Li, S. Measuring land change in coastal zone around a rapidly urbanized bay. *Int. J. Environ. Res. Public Health* **2018**, *15*, 1059. [[CrossRef](#)]
- Pourebahim, S.; Hadipour, M.; Bin Mokhtar, M. Impact assessment of rapid development on land-use changes in coastal areas; case of Kuala Langat district, Malaysia. *Environ. Dev. Sustain.* **2015**, *17*, 1003–1016. [[CrossRef](#)]
- Kourosh Niya, A.; Huang, J.; Kazemzadeh-Zow, A.; Naimi, B. An adding/deleting approach to improve land change modeling: A case study in Qeshm Island, Iran. *Arab. J. Geosci.* **2019**, *12*, 333. [[CrossRef](#)]
- Ramesh, R.; Chen, Z.; Cummins, V.; Day, J.; D’Elia, C. Land–Ocean Interactions in the Coastal Zone: Past, present & future. *Anthropocene* **2015**, *12*, 85–98.
- Huang, J.; Pontius, R.G., Jr.; Li, Q.; Zhang, Y. Use of intensity analysis to link patterns with processes of land change from 1986 to 2007 in a coastal watershed of southeast China. *Appl. Geogr.* **2012**, *34*, 371–384. [[CrossRef](#)]
- Kuemmerle, T.; Erb, K.; Meyfroidt, P.; Müller, D.; Verburg, P.H.; Estel, S.; Haberl, H.; Hostert, P.; Jepsen, M.R.; Kastner, T.; et al. Challenges and opportunities in mapping land use intensity globally. *Curr. Opin. Environ. Sustain.* **2013**, *5*, 484–493. [[CrossRef](#)]
- Mohajane, M.; Essahlaoui, A.; Oudija, F.; Hafyani, M.E.; Hmaid, A.E.; Ouali, A.E.; Randazzo, G.; Teodoro, A.C. Land Use/Land Cover (LULC) Using Landsat Data Series (MSS, TM, ETM+ and OLI) in Azrou Forest, in the Central Middle Atlas of Morocco. *Environments* **2018**, *5*, 131. [[CrossRef](#)]
- Msofe, N.K.; Sheng, L.; Lyimo, J. Land Use Change Trends and Their Driving Forces in the Kilombero Valley Floodplain, South eastern Tanzania. *Sustainability* **2019**, *11*, 505. [[CrossRef](#)]
- Schaller, J.; Mattos, C. GIS Model Applications for Sustainable Development and Environmental Planning at the Regional Level. In *GeoSpatial Visual Analytics*; Amicis, R.D., Stojanovic, R., Conti, G., Eds.; NATO Science for Peace and Security Series C: Environmental Security; Springer: Dordrecht, The Netherlands, 2009.
- Aldwaik, S.Z.; Pontius, R.G. Intensity analysis to unify measurements of size and stationarity of land changes by interval, category, and transition. *Landsc. Urban Plan* **2012**, *106*, 103–114. [[CrossRef](#)]
- Mwangi, H.M.; Lariu, P.; Julich, S.; Patil, S.D.; McDonald, M.A.; Feger, K.-H. Characterizing the Intensity and Dynamics of Land-Use Change in the Mara River Basin, East Africa. *Forests* **2018**, *9*, 8. [[CrossRef](#)]
- Quan, B.; Ren, H.; Pontius, R.G., Jr.; Liu, P. Quantifying spatiotemporal patterns concerning land change in Changsha, China. *Landsc. Ecol. Eng.* **2018**, *14*, 257–267. [[CrossRef](#)]
- Pontius, R.G., Jr.; Gao, Y.; Giner, N.M.; Kohyama, T.; Osaki, M.; Hirose, K. Design and Interpretation of Intensity Analysis Illustrated by Land Change in Central Kalimantan, Indonesia. *Land* **2013**, *2*, 351–369. [[CrossRef](#)]
- Zhou, P.; Huang, J.; Pontius, J.G.R.; Hong, H. Land Classification and Change Intensity Analysis in a Coastal Watershed of Southeast China. *Sensors* **2014**, *14*, 11640–11658. [[CrossRef](#)] [[PubMed](#)]
- Akinyemi, F.O.; Pontius, R.G., Jr.; Braimoh, A.K. Land change dynamics: Insights from Intensity Analysis applied to an African emerging city. *J. Spat. Sci.* **2016**, *62*, 69–83. [[CrossRef](#)]
- Shoyama, K.; Braimoh, A.K.; Avtar, R.; Saito, O. Land Transition and Intensity Analysis of Cropland Expansion in Northern Ghana. *Environ. Manag.* **2018**, *62*, 892–905. [[CrossRef](#)]

20. Da, F.; Chen, X.; Qi, J. Spatiotemporal Characteristic of Land Use/Land Cover Changes in the Middle and Lower Reaches of Shule River Basin Based on an Intensity Analysis. *Sustainability* **2019**, *11*, 1360. [[CrossRef](#)]
21. Huang, B.; Huang, J.; Pontius, R.G., Jr.; Tu, Z. Comparison of Intensity Analysis and the land-use dynamic degrees to measure land changes outside versus inside the coastal zone of Longhai, China. *Ecol. Indic.* **2018**, *89*, 336–347. [[CrossRef](#)]
22. Sarvar, R.; Khaliji Oskouei, M.A. The role of Qeshm city in the regional economy development. *J. Urban Econ. Manag.* **2014**, *2*, 53–67.
23. Financial Tribune, Qeshm Island: Persian Gulf Commercial Hub. 2015. Available online: <https://financialtribune.com/articles/economy-domestic-economy/12704/qeshm-island-persian-gulf-commercial-hub> (accessed on 7 March 2015).
24. Mohammadi Mazraeh, H.; Pazhouhanfar, M. Effects of vernacular architecture structure on urban sustainability case study: Qeshm Island, Iran. *Front. Archit. Res.* **2018**, *7*, 11–24. [[CrossRef](#)]
25. Mirza, R.; Moeinaddini, M.; Pourebrahim, S.; Zahed, M.A. Contamination, ecological risk and source identification of metals by multivariate analysis in surface sediments of the khouran Straits, the Persian Gulf. *Mar. Poll. Bull.* **2019**, *145*, 526–535. [[CrossRef](#)]
26. Pourahmad, A.; Hosseini, A.; Pourahmad, A.; Zoghi, M.; Sadat, M. Tourist Value Assessment of Geotourism and Environmental Capabilities in Qeshm Island-Iran. *Geoheritage* **2018**, *10*, 687–706. [[CrossRef](#)]
27. Keshtkar, H.; Voigt, W. Potential impacts of climate and landscape fragmentation changes on plant distributions: Coupling multi-temporal satellite imagery with gis-based cellular automata model. *Ecol. Inform.* **2016**, *32*, 145–155. [[CrossRef](#)]
28. Richards, J.A. *Remote Sensing Digital Image Analysis*, 5th ed.; Springer: Berlin, Germany, 2013.
29. Li, C.; Wang, J.; Wang, L.; Hu, L.; Gong, P. Comparison of Classification Algorithms and Training Sample Sizes in Urban Land Classification with Landsat Thematic Mapper Imagery. *Remote Sens.* **2014**, *6*, 964–983. [[CrossRef](#)]
30. Millard, K.; Richardson, M. On the Importance of Training Data Sample Selection in Random Forest Image Classification: A Case Study in Peatland Ecosystem Mapping. *Remote Sens.* **2015**, *7*, 8489–8515. [[CrossRef](#)]
31. Abdu, H.A. Classification accuracy and trend assessments of land cover- land use changes from principal components of land satellite images. *Int. J. Remote Sens.* **2019**, *40*, 1275–1300. [[CrossRef](#)]
32. Foody, G. Status of land covers classification accuracy assessment. *Remote Sens. Environ.* **2002**, *1*, 185–201. [[CrossRef](#)]
33. Zaehringer, J.G.; Eckert, S.; Messerli, P. Revealing Regional Deforestation Dynamics in North-Eastern Madagascar—Insights from Multi-Temporal Land Cover Change Analysis. *Land* **2015**, *4*, 454–474. [[CrossRef](#)]
34. Aldwaik, S.Z.; Pontius, R.G., Jr. Map errors that could account for deviations from a uniform intensity of land change. *Int. J. Geogr. Inf. Sci.* **2013**, *27*, 1717–1739. [[CrossRef](#)]
35. Enaruvbe, G.O.; Pontius, R.G., Jr. Influence of classification errors on Intensity Analysis of land changes in southern Nigeria. *Int. J. Remote Sens.* **2015**, *36*, 244–261. [[CrossRef](#)]
36. Mafi-Gholami, D.; Zenner, E.K.; Jaafari, A.; Ward, R.D. Modeling multi-decadal mangrove leaf area index in response to drought along the semi-arid southern coasts of Iran. *Sci. Total Environ.* **2019**, *656*, 1326–1336. [[CrossRef](#)]
37. Zuo, L.J.; Xu, J.Y.; Zhang, Z.X. Spatial temporal land use change and landscape response in Bohai Sea coastal zone area. *J. Remote Sens.* **2011**, *15*, 604–620. (In Chinese)
38. Yang, Y.; Liu, Y.; Xu, D. Use of intensity analysis to measure land use changes from 1932 to 2005 in Zhenlai County, Northeast China. *Chin. Geogr. Sci.* **2017**, *27*, 441–455. [[CrossRef](#)]
39. Khorani, A.; Bineiaz, M.; Amiri, H.R. Mangrove forest area changes due to climatic changes (Case study: Forest between the port and the Khamir island). *J. Aquat. Ecol.* **2015**, *5*, 100–111. (In Persian with English abstract)
40. Liu, J.; Liu, M.; Zhuang, D.; Zhang, Z.; Deng, X. Study on spatial pattern of land-use change in China during 1995–2000. *Sci. China Ser. D Earth Sci.* **2003**, *46*, 373–384.
41. Badmos, O.S.; Rienow, A.; Callo-Concha, D.; Greve, K.; Jürgens, C. Urban Development in West Africa—Monitoring and Intensity Analysis of Slum Growth in Lagos: Linking Pattern and Process. *Remote Sens.* **2018**, *10*, 1044. [[CrossRef](#)]
42. Munsu, M.; Malaviya, S.; Oinam, G. A landscape approach for quantifying land-use and land-cover change (1976–2006) in middle Himalaya. *Reg. Environ. Chang.* **2010**, *10*, 145. [[CrossRef](#)]

43. Hakimian, H. Iran's Free Trade Zones: Challenges and Opportunities. In *Iran's Economy at a Crossroads: Domestic and Global Challenges*; University of Southern California (USC): Los Angeles, CA, USA, 2009.
44. Ministry of the Interior of the Islamic Republic of Iran. *Annual Statistical Report*; Ministry of the Interior of the Islamic Republic of Iran: Hormozgan Province, Iran, 2016.
45. Zarei, M.; Fatemi, M.R.; Mortazavi, M.S.; Pourebrahim, S.; Ghoddousi, J. Selection of the optimal tourism site using the ANP and fuzzy TOPSIS in the framework of Integrated Coastal Zone Management: A case of Qeshm Island. *Ocean Coast Manag.* **2016**, *130*, 179–187.
46. Masnavi, M.R.; Amani, N.; Ahmadzadeh, A. Ecological Landscape Planning and Design Strategies for Mangrove Communities (Hara Forests) in South-Pars Special Economic Energy Zone, Asalouyeh-Iran. *Environ. Nat. Resour. Res.* **2016**, *6*. [[CrossRef](#)]



© 2019 by the authors. Licensee MDPI, Basel, Switzerland. This article is an open access article distributed under the terms and conditions of the Creative Commons Attribution (CC BY) license (<http://creativecommons.org/licenses/by/4.0/>).